

## Electron mobility enhancement in ZnO thin films via surface modification by carboxylic acids

Josef W. Spalenka, Padma Gopalan, Howard E. Katz, and Paul G. Evans

Citation: *Appl. Phys. Lett.* **102**, 041602 (2013); doi: 10.1063/1.4790155

View online: <http://dx.doi.org/10.1063/1.4790155>

View Table of Contents: <http://apl.aip.org/resource/1/APPLAB/v102/i4>

Published by the [American Institute of Physics](http://www.aip.org).

---

### Related Articles

Investigation of electrical transport in anodized single TiO<sub>2</sub> nanotubes

*Appl. Phys. Lett.* **102**, 043105 (2013)

Detecting the local transport properties and the dimensionality of transport of epitaxial graphene by a multi-point probe approach

*Appl. Phys. Lett.* **102**, 033110 (2013)

Piezoresistance of nano-scale silicon up to 2GPa in tension

*Appl. Phys. Lett.* **102**, 031911 (2013)

Electrical transport and photocurrent mechanisms in silicon nanocrystal multilayers

*J. Appl. Phys.* **113**, 043703 (2013)

Stochastic nonlinear electrical characteristics of graphene

*Appl. Phys. Lett.* **102**, 033101 (2013)

---

### Additional information on *Appl. Phys. Lett.*

Journal Homepage: <http://apl.aip.org/>

Journal Information: [http://apl.aip.org/about/about\\_the\\_journal](http://apl.aip.org/about/about_the_journal)

Top downloads: [http://apl.aip.org/features/most\\_downloaded](http://apl.aip.org/features/most_downloaded)

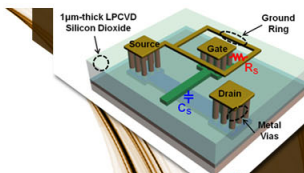
Information for Authors: <http://apl.aip.org/authors>

## ADVERTISEMENT



**EXPLORE WHAT'S  
NEW IN APL**

**SUBMIT YOUR PAPER NOW!**



### **SURFACES AND INTERFACES**

Focusing on physical, chemical, biological, structural, optical, magnetic and electrical properties of surfaces and interfaces, and more...



### **ENERGY CONVERSION AND STORAGE**

Focusing on all aspects of static and dynamic energy conversion, energy storage, photovoltaics, solar fuels, batteries, capacitors, thermoelectrics, and more...

## Electron mobility enhancement in ZnO thin films via surface modification by carboxylic acids

Josef W. Spalenska,<sup>1</sup> Padma Gopalan,<sup>1,2</sup> Howard E. Katz,<sup>3</sup> and Paul G. Evans<sup>1,2,a)</sup>

<sup>1</sup>Materials Science Program, University of Wisconsin, Madison, Wisconsin 53706, USA

<sup>2</sup>Department of Materials Science and Engineering, University of Wisconsin, Madison, Wisconsin 53706, USA

<sup>3</sup>Department of Materials Science and Engineering, Johns Hopkins University, Baltimore, Maryland 21218, USA

(Received 24 October 2012; accepted 18 January 2013; published online 29 January 2013)

Modifying the surface of polycrystalline ZnO films using a monolayer of organic molecules with carboxylic acid attachment groups increases the field-effect electron mobility and zero-bias conductivity, resulting in improved transistors and transparent conductors. The improvement is consistent with the passivation of defects via covalent bonding of the carboxylic acid and is reversible by exposure to a UV-ozone lamp. The properties of the solvent used for the attachment are crucial because solvents with high acid dissociation constants ( $K_a$ ) for carboxylic acids lead to high proton activities and etching of the nanometers-thick ZnO films, masking the electronic effect.

© 2013 American Institute of Physics. [<http://dx.doi.org/10.1063/1.4790155>]

Among inorganic semiconductors for large-area photovoltaics and transparent electronics, ZnO is particularly attractive because it is composed of non-toxic, low cost, earth abundant elements, easily forms films and nanostructures by room-temperature solution processing,<sup>1</sup> and has high transparency in the visible spectrum.<sup>2</sup> Production of ZnO thin films with excellent electronic properties, however, often involves either vacuum deposition techniques, such as rf magnetron sputtering<sup>3</sup> or high-temperature post-processing steps that are incompatible with flexible substrates that degrade at high temperatures. The fabrication of electronic materials nearer to room temperature, on flexible substrates, and without vacuum processing would be valuable in electronic applications. Transparent conducting films based on semiconducting ZnO layers grown and deposited from solutions can be an important component of low-cost solar cells, transparent electrodes for large-area lighting panels, and the transparent circuit elements that drive the pixels in emerging display technologies such as organic light-emitting diode displays.

The electronic properties of ZnO layers created from solution-deposited precursors are initially dominated by defects and impurities.<sup>4</sup> As a result, the properties of these layers are often subsequently enhanced via high-temperature processing steps. Common strategies include annealing in either hydrogen gas environments<sup>5,6</sup> or in the presence of a hydrogen-rich capping layer,<sup>7</sup> which increases the carrier concentration by introducing hydrogen into the ZnO and creates shallow donor states.<sup>8</sup> Removing oxygen-vacancy donor states by annealing in an oxygen-rich environment has the opposite effect, reducing the carrier concentration.<sup>9</sup> These high-temperature processing steps, typically at 350–600 °C, are not compatible with flexible polymer substrates, such as polyethylene terephthalate (PET) and polyethylene naphthalate (PEN), which are mechanically and chemically unstable above 200 °C.<sup>10,11</sup> Therefore, strategies for enhancing the field-effect electron mobility and conductivity of ZnO films at low temperatures with solution-based methods are desirable. Here, we show that chemical functionalization of the surface

of a thin ZnO film can have a dramatic effect on its electronic properties. Chemical modification of semiconductor interfaces has already had an important role in extending the scope of application of other semiconductors. Passivating the dangling bonds at Si/SiO<sub>2</sub> interfaces with deuterium instead of hydrogen, for example, extends the lifetime of metal-oxide-silicon devices by reducing the generation of defects by hot electrons.<sup>12</sup> Similarly, surface treatments of ZnO films could become an integral part of producing ZnO-based devices.

The electronic and physical properties of interfaces between ZnO and other materials can be changed by modifying the surface of ZnO with covalently bonded organic monolayers.<sup>13,14</sup> Molecules attached to the surface of ZnO are used to change the wetting properties of liquids and to improve the ordering of subsequently deposited layers of polymers and small molecules.<sup>13,14</sup> Surfaces of ZnO nanowires functionalized with stearic acid (CH<sub>3</sub>(CH<sub>2</sub>)<sub>16</sub>COOH) exhibit superhydrophobicity and are more stable in aqueous environments than bare ZnO nanowires.<sup>15–17</sup> Modifying the surface of ZnO with organic monolayers can also result in changes in electronic properties. The effects of surface layers on charge transfer from organic semiconductors to ZnO depend on the electronic structure of the monolayer. The wide energy gap between the highest occupied molecular orbital and lowest unoccupied molecular orbital of stearic acid impedes the transport of carriers.<sup>18</sup> The increased ordering of poly 3-hexylthiophene (P3HT) films on alkane-functionalized ZnO results in an improvement in the efficiency of P3HT/ZnO solar cells, enough to offset the detrimental effects due to the creation of the intermediate insulating alkane layer.<sup>19</sup> In these examples, the direction of current transport is normal to the plane of the ZnO surface. We expect that molecules grafted to the surface of ZnO will also change the electronic properties of the near-surface region of ZnO, and thus modify electronic transport within ZnO.

Here, we show that the attachment of molecules linked by carboxylic acid groups to the surface of a ZnO thin film increases the field-effect mobility of electrons. We demonstrate this effect in solution-deposited polycrystalline ZnO films, which form the channel of field-effect transistors

<sup>a)</sup>Electronic mail: [evans@engr.wisc.edu](mailto:evans@engr.wisc.edu).

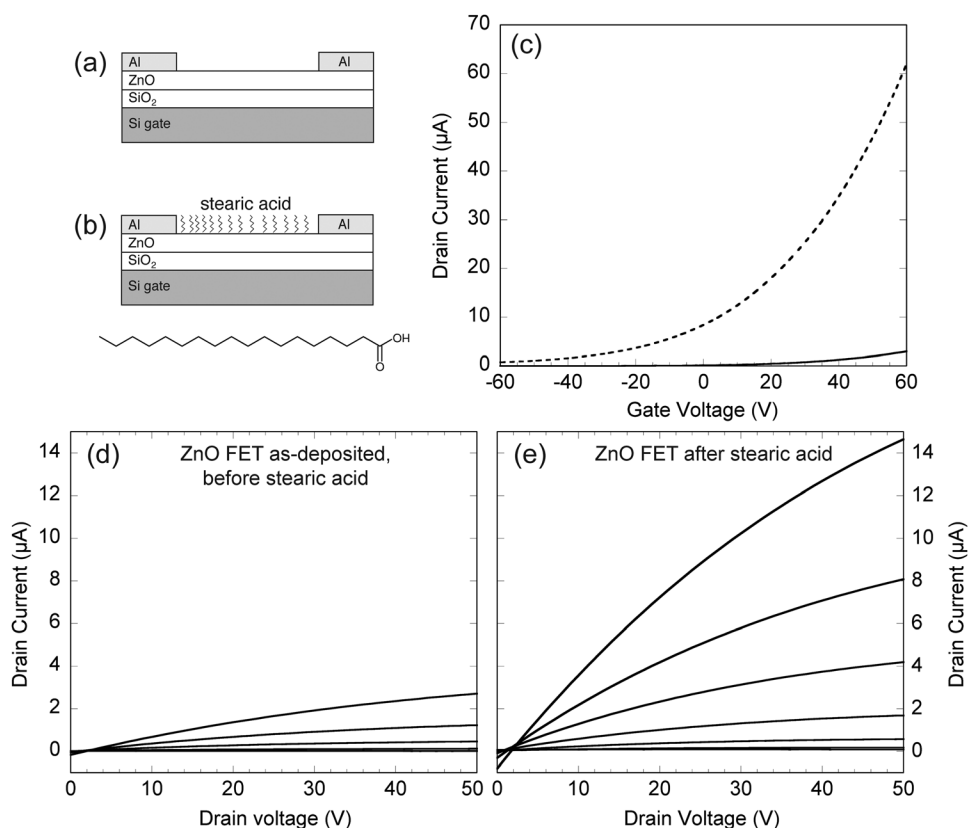


FIG. 1. Solution-deposited ZnO FET (a) as-deposited and (b) after the attachment structure of the stearic acid layer. The chemical structure of stearic acid is shown in (b). (c) Drain current as a function of gate voltage for an as-deposited ZnO FET (solid curve) and for the same device after surface treatment with stearic acid (dashed curve). Output characteristics of the ZnO FETs (d) before and (e) after surface treatment with stearic acid. The gate voltage increases in steps of 20 V from  $-60$  V (off) to  $+60$  V (on).

(FETs). We compare FETs fabricated from the as-deposited ZnO film, shown in Figure 1(a), to FETs in which the ZnO is subsequently functionalized using stearic acid, Figure 1(b). An increase in electron mobility leads to an increase in the conductivity of the thin polycrystalline ZnO films. The effect persists at zero gate bias in FETs and thus would also be present in ungated ZnO layers.

ZnO films were deposited by spin coating a precursor solution onto substrates consisting of 300 nm  $\text{SiO}_2$  on highly doped silicon, which served as the gate dielectric and bottom gate, respectively. The precursor solution consisted of 0.3 M zinc acetate dihydrate in absolute ethanol with 0.3 M of acetylacetone added as a stabilizer. The precursor solution was stirred overnight at room temperature and filtered through a  $0.2 \mu\text{m}$  polytetrafluoroethylene filter prior to spin coating. The substrates were pre-cleaned in a 3:1 mixture of sulfuric acid and hydrogen peroxide for 5 min, which was heated to approximately  $80^\circ\text{C}$  by the exothermic reaction that occurs upon mixing the solution. The substrates were then sonicated for 5 min each in acetone, isopropyl alcohol, and water. The ZnO precursor was deposited onto the  $\text{SiO}_2$  by spin coating at 5000 revolutions per min for 30 s followed by heating to  $75^\circ\text{C}$  for 10 min to evaporate residual solvent. The coating process was then repeated. The films were annealed in air in a quartz tube furnace at  $450^\circ\text{C}$  for 75 min. Surface treatments similar to the one we describe below would apply to ZnO grown by methods involving even lower temperatures, such as chemical bath deposition<sup>20</sup> and decomposition of low-temperature inorganic inks, which have been shown to crystallize at temperatures as low as  $150^\circ\text{C}$ .<sup>21</sup> Source and drain top contacts were formed by depositing Al films with a thickness of 100 nm by electron-beam evaporation through a shadow mask with channel lengths and width of  $100 \mu\text{m}$  and

$1000 \mu\text{m}$ , respectively. The ZnO exhibits a crystallographic texture in which the c-axis is along the surface normal of the substrate. X-ray diffraction  $\theta$ - $2\theta$  scans over an angular range in which the ZnO 100, 002, 101, and 102 reflections would occur exhibit only the 002 reflection. A similar crystallographic texture is observed in other solution-deposited ZnO films on smooth  $\text{SiO}_2$  surfaces.<sup>22</sup>

A self-assembled monolayer of stearic acid was added to the ZnO surface by immersing the ZnO FETs in a 1 mM solution of stearic acid in tetrahydrofuran (THF) at room temperature for 2 h. The use of THF is critical because the acid dissociation constant ( $K_a$ ) is smaller ( $pK_a$  larger) for carboxylic acids in THF than in other common solvents. Higher  $pK_a$  corresponds to less acidic solutions, which etch the ZnO surface more slowly. Values of  $pK_a$  for acetic acid, a simple molecule with a carboxylic acid group, in common solvents used for functionalizing ZnO are collected from the literature and summarized in Table I.<sup>23-26</sup> The values of  $pK_a$  for acetic acid provide insight into what can be expected with more complex carboxylic acids, for which the dissociation constants are not yet available. Table I also illustrates the expected correlation of  $pK_a$  with the relative dielectric constant  $\epsilon_r$  of the solvent and gives  $\text{H}^+$  ion concentrations for experimentally relevant functionalization solutions. The expected concentration of dissociated hydrogen ions is more than 5 orders of magnitude lower in THF than in ethanol, dimethyl sulfoxide (DMSO), or dimethylformamide (DMF). The  $pK_a$  is sufficiently high in THF that ZnO films with nanometer thicknesses can be immersed in THF/carboxylic acid solutions for as long as three days with no etching of the ZnO surface apparent in optical microscopy. The same concentration of carboxylic acid in ethanol, DMSO, or DMF completely dissolves the ZnO in the same time. A similar strategy

TABLE I. pKa, molecular dipole moment, dielectric constant  $\epsilon_r$ , and hydrogen ion concentration under common carboxylic acid attachment conditions for acetic acid solutions in solvents used for ZnO surface functionalization. The pKa and dielectric constants are from Ref. 23 for acetonitrile and THF, and from Ref. 25 for other solvents. The pKa are taken from Ref. 26 for DMSO and DMF and from Ref. 24 for other solvents. The dipole moments are from Ref. 24.

Solvent	pKa (acetic acid)	$[H^+]$ for 1 mM acetic acid (M)	Dipole moment (D)	$\epsilon_r$
H <sub>2</sub> O	4.76	$1 \times 10^{-4}$	1.85	80
Methanol	9.7	$4 \times 10^{-7}$	1.70	33
Ethanol	10.3	$2 \times 10^{-7}$	1.69	24
DMSO	12.6	$2 \times 10^{-8}$	3.96	49
DMF	13.5	$6 \times 10^{-9}$	3.86	37
Acetonitrile	22.3	$2 \times 10^{-13}$	3.92	36
THF	24	$3 \times 10^{-14}$	1.75	7.6

is required to create carboxylic-acid linked layers of other molecules.<sup>18,27</sup> Atomic force microscopy (AFM) images of the surface of the ZnO layer before the functionalization with stearic acid reveal that the ZnO films consist of 25–75 nm diameter crystals. Line profiles extracted from the images indicate that the height of the surface varies over a range of less than 10 nm both before and after addition of the stearic acid layer. There is no apparent change in the number density or diameter of the nanocrystals after functionalization.

Figure 1(c) shows the drain current as a function of gate voltage for a ZnO FET before (solid curve) and after (dashed curve) the creation of the stearic acid layer. The saturation field-effect electron mobility increases from  $0.01 \text{ cm}^2 \text{ V}^{-1} \text{ s}^{-1}$  in the as-deposited FET to  $0.13 \text{ cm}^2 \text{ V}^{-1} \text{ s}^{-1}$  after attachment of stearic acid to the surface. Figures 1(d) and 1(e) show the output characteristics in which the drain current is measured as a function of drain voltage  $V_d$  at a series of different gate voltages, for a representative transistor before and after functionalization with stearic acid. In addition to the increased source-drain current after stearic acid functionalization, Figure 1(e) also exhibits a small non-zero current at  $V_d = 0$ , arising from gate leakage at high gate voltages. Electrical measurements were made in the dark in order to eliminate possible contributions to the source-drain current due to photocurrent<sup>28</sup> or a light-induced threshold voltage shift.<sup>29</sup> Because of differences in film thickness and thermal post-treatment, the field-effect mobility reported here is not among the highest found in the literature for solution processed ZnO, in which mobilities as high as  $6 \text{ cm}^2 \text{ V}^{-1} \text{ s}^{-1}$  have been reported.<sup>30</sup> However, the relative increase in the field-effect mobility that can be attributed to the stearic acid treatment is significant and could place ultra-thin and lower-temperature processed ZnO films into a technologically relevant regime.

The zero gate bias conductivity was extracted from measurements of the conductance using the slope of the  $I_d$  versus  $V_d$  plots in Figures 1(d) and 1(e). The slopes were measured in the linear region of transistor operation, with  $V_d$  less than 10 V. The conductivity is calculated from the conductance assuming that the electrons responsible for conduction are uniformly distributed throughout the 25 nm thick ZnO film. The corresponding effective resistivity of the channel decreases by an order of magnitude from an initial value of  $4.5 \times 10^3 \text{ } \Omega \text{ cm}$

to  $4.2 \times 10^2 \text{ } \Omega \text{ cm}$  after functionalization with the stearic acid monolayer. Undoped ZnO layers with thicknesses less than 50 nm typically have very high resistivities of more than  $10^3 \text{ } \Omega \text{ cm}$ . Introducing the stearic acid layer yields undoped ZnO films with resistivities comparable to what can be achieved by doping or by annealing in hydrogen.<sup>31,32</sup>

Mechanisms that could potentially contribute to the increased field-effect electron mobility include (1) etching of the ZnO surface, eliminating defects, (2) passivation of defect scattering sites by covalent bonding of the carboxylic acid groups to defects, resulting in direct chemical passivation or a beneficial local electric field, and (3) the incorporation of the hydrogen released from the carboxylic acid group into the ZnO film, accompanied by a reductive process, where H could act as a dopant. To investigate the possibility that the increased mobility results from etching that eliminates surface defects, a control experiment was performed in which ZnO FETs were subjected to treatments in a dilute inorganic acid to etch the surface. A ZnO FET was immersed in increasingly acidic HCl solutions for 10 min, rinsed with clean THF, and dried with a nitrogen gun. Hydrochloric acid was selected for the control experiments because unlike stearic acid, the  $\text{Cl}^-$  anion in HCl does not covalently bond to the ZnO surface in the same manner as a carboxylic acid group. The drain current was measured as a function of gate voltage between each immersion step in the etching experiment. As shown in Figure 2, mild etching of ZnO film with the dilute HCl solutions consistently decreases the conductivity of the films. This etching experiment exhibits the opposite effect as is found in the case of carboxylic acid surface functionalization, and we thus eliminate the possibility that etching contributes to the improvement of the field-effect mobility.

If the electronic effect on the ZnO is due to the carboxylic acid binding chemistry, rather than physical changes to the ZnO structure by etching or incorporation of hydrogen

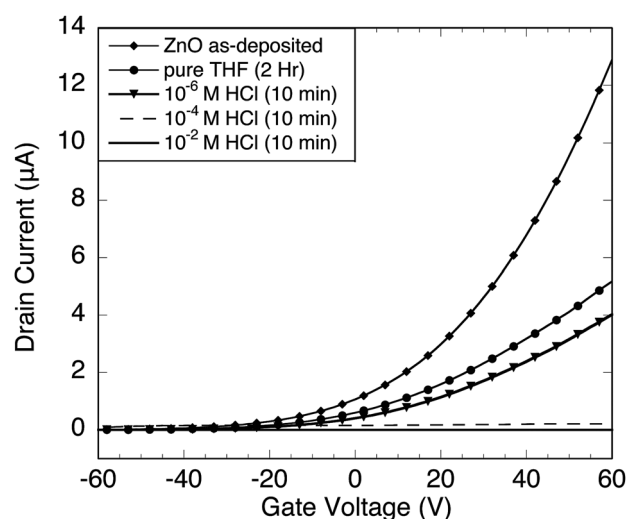


FIG. 2. Drain current as a function of gate voltage for a ZnO FET after etching in dilute solutions of HCl in THF. The as-deposited ZnO device (diamonds) has the highest current. The source-drain current decreases after immersion in pure THF for 2 h (circles) and continues to decrease after 10 min immersion in solutions of HCl in THF with concentrations of  $10^{-6}$  M (triangles) and  $10^{-4}$  M (dashed line). The channel is completely removed after 10 min. in a solution of  $10^{-2}$  M HCl in THF (solid line).

atoms into the ZnO lattice, it should be reversible by removing the organic molecules from the surface. To investigate the potential reversibility of the observed electronic effect, the FET structures were placed within 5 mm of an ozone-producing ultraviolet lamp after the stearic acid surface treatment. The combination of UV photons and ozone breaks C-C bonds in organic molecules and converts the molecular fragments to volatile species that leave the surface, comprising an effective room-temperature, dry cleaning method for removing organic surface molecules.<sup>33</sup>

The transfer characteristics of a ZnO FET device (Figure 3(a)) and the drain current as a function of drain voltage at  $V_g = 0$  (Figure 3(b)) were measured after sequentially alternating treatments of a single ZnO FET sample between a UV-ozone lamp and the stearic acid treatment. After each round of stearic acid treatment, the samples were found to be hydrophobic, and after UV-ozone treatment, the samples became hydrophilic, as observed by placing a drop of deionized water on the ZnO film surface. Figure 3(a) shows the initial transfer characteristics of a ZnO FET sample, which had been stored in ambient conditions for several weeks (1),

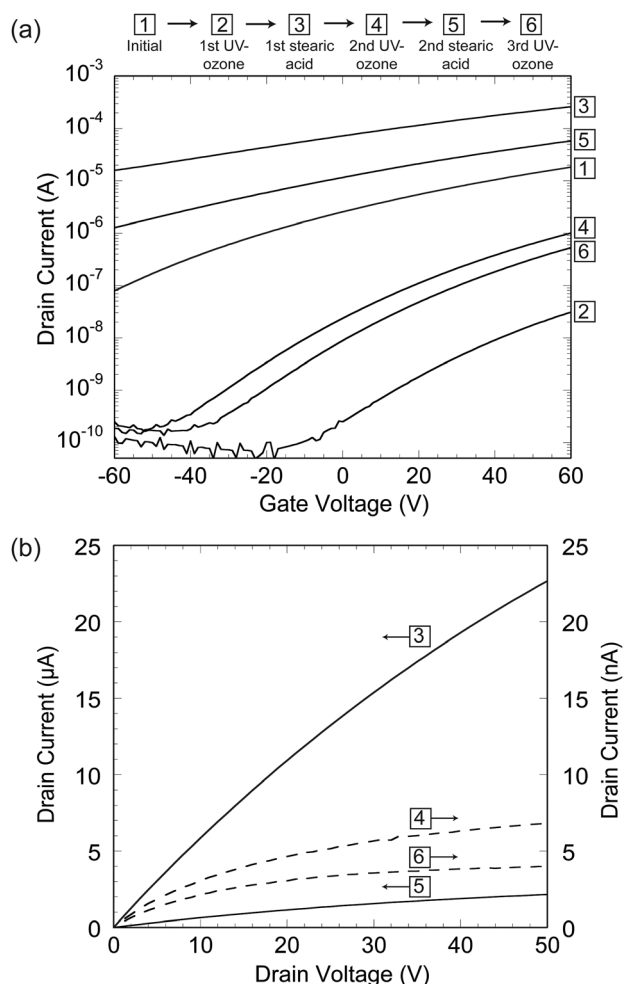


FIG. 3. (a) Transfer curves of a single ZnO FET device measured after alternating surface treatments of stearic acid and UV-ozone showing the reversibility of the carboxylic acid electronic effect. The numbered boxes indicate the sequence of the surface treatments. (b) The zero gate bias drain current as a function of drain voltage after alternating treatments with stearic acid (solid curves, left axis) and UV-ozone exposure (dashed curves, right axis). The scale for the left y-axis ( $\mu$ A) is a factor of  $10^3$  larger than the right axis (nA).

then exposed to a UV-ozone lamp for 5 min and re-measured within 5 min of the end of exposure (2). The FET was then functionalized following the previously described procedure in a 1 mmol stearic acid solution (3), and again exposed to the UV-ozone lamp for 5 min (4). The stearic acid and UV ozone treatments were then repeated once more each (5) and (6). The drain current at all gate voltages is several orders of magnitude higher for the ZnO FET when the stearic acid layer is present, compared to the device after it is exposed to UV-ozone.

Figure 3(b) shows the drain current as a function of drain voltage at zero gate voltage for the sample after stearic acid treatments (solid curves, left y-axis), and after 5 min UV-ozone exposures (dashed curves, right y-axis). The resistivity of the ZnO functionalized with stearic acid,  $43 \Omega \text{ cm}$ , is increased by a factor of 2000 to  $8.3 \times 10^4 \Omega \text{ cm}$  by removal of the surface layer with the UV-ozone treatment. We note that the resistivity of the ZnO devices with stearic acid is lowest if the film is first pre-treated with UV-ozone. This is presumably due to an increase in potential sites for carboxylic acid attachment that become available after the UV-ozone cleaning treatment.

The interaction between UV-ozone and the ZnO film is itself a complex process and includes several competing effects such as the creation of additional oxygen interstitials or the removal of oxygen vacancies, both of which can reduce the ZnO conductivity with increasing UV-ozone dose, separate from the effects of removing the organic molecules from the surface.<sup>34</sup> However, we can conclude that the attachment of the organic layer is the dominant effect in restoring the high conductivity state, because the stearic acid solution treatment is not expected to significantly alter the concentrations of either oxygen vacancies or oxygen interstitials in the film.

The improved conductivity induced by stearic acid will be particularly important in devices requiring thin oxide semiconductor layers, for example, in flexible electronic devices. In addition, transport in the oxide phase of composite structures such as dye-sensitized solar cells (DSSCs) can be potentially improved by appropriate functionalization of the oxide surface. The dyes already used in DSSCs rely on carboxylic acid attachment chemistry to anchor dye molecules.<sup>35</sup> Our results show that the carboxylic acid group may have a constructive effect in its own right, besides acting as an anchor for the dyes. More broadly, the identification of lower-pKa media for carboxylic attachment to oxides broadens the scope of monolayer attachment chemistries available to acid-etchable oxide substrates.

This work was supported by the University of Wisconsin Materials Research Science and Engineering Center, NSF Grant No. DMR-1121288.

<sup>1</sup>Z. R. Tian, J. A. Voigt, J. Liu, B. McKenzie, M. J. McDermott, M. A. Rodriguez, H. Konishi, and H. Xu, *Nature Mater.* **2**, 821 (2003).

<sup>2</sup>R. L. Hoffman, B. J. Norris, and J. F. Wager, *Appl. Phys. Lett.* **82**, 733 (2003).

<sup>3</sup>E. M. C. Fortunato, P. M. C. Barquinha, A. C. M. B. G. Pimentel, A. M. F. Gonçalves, A. J. S. Marques, L. M. N. Pereira, and R. F. P. Martins, *Adv. Mater.* **17**, 590 (2005).

- <sup>4</sup>K. H. Tam, C. K. Cheung, Y. H. Leung, A. B. Djuricic, C. C. Liang, C. D. Beling, S. Fung, W. M. Kwok, D. L. Phillips, L. Ding, and W. K. Ge, *J. Phys. Chem. B* **110**, 20865 (2006).
- <sup>5</sup>B.-Y. Oh, M.-C. Jeong, D.-S. Kim, W. Lee, and J.-M. Myoung, *J. Cryst. Growth* **281**, 475 (2005).
- <sup>6</sup>Y. Natsume and H. Sakata, *J. Mater. Sci.: Mater. Electron.* **12**, 87 (2001).
- <sup>7</sup>M. V. Ponomarev, K. Sharma, M. A. Verheijen, M. C. M. van de Sanden, and M. Creatore, *J. Appl. Phys.* **111**, 063715 (2012).
- <sup>8</sup>C. G. Van de Walle, *Phys. Rev. Lett.* **85**, 1012 (2000).
- <sup>9</sup>B. Lin, Z. Fu, and Y. Jia, *Appl. Phys. Lett.* **79**, 943 (2001).
- <sup>10</sup>R. C. Hoffmann, S. Dilfer, A. Issanin, and J. J. Schneider, *Phys. Status Solidi A* **207**, 1590 (2010).
- <sup>11</sup>Y. Sun and J. A. Rogers, *Adv. Mater.* **19**, 1897 (2007).
- <sup>12</sup>K. Hess, I. Kizilyalli, and J. W. Lyding, *IEEE Trans. Electron Devices* **45**, 406 (1998).
- <sup>13</sup>C. G. Allen, D. J. Baker, J. M. Albin, H. E. Oertli, D. T. Gillaspie, D. C. Olson, T. E. Furtak, and R. T. Collins, *Langmuir* **24**, 13393 (2008).
- <sup>14</sup>T. C. Monson, M. T. Lloyd, D. C. Olson, Y.-J. Lee, and J. W. P. Hsu, *Adv. Mater.* **20**, 4755 (2008).
- <sup>15</sup>C. Badre, T. Pauporté, M. Turmine, and D. Lincot, *Nanotechnology* **18**, 365705 (2007).
- <sup>16</sup>G. Kwak, M. Seol, Y. Tak, and K. Yong, *J. Phys. Chem. C* **113**, 12085 (2009).
- <sup>17</sup>C. Lao, C. P. Wong, and Z. L. Wang, *Nano Lett.* **7**, 1323 (2007).
- <sup>18</sup>J. W. Spalenka, P. Paoprasert, R. Franking, R. J. Hamers, P. Gopalan, and P. G. Evans, *Appl. Phys. Lett.* **98**, 103303 (2011).
- <sup>19</sup>C. G. Allen, D. J. Baker, T. M. Brenner, C. C. Weigand, J. M. Albin, K. X. Steirer, D. C. Olson, C. Ladam, D. S. Ginley, R. T. Collins, and T. E. Furtak, *J. Phys. Chem. C* **116**, 8872 (2012).
- <sup>20</sup>S.-H. Yi, S.-K. Choi, J.-M. Jang, J.-A. Kim, and W.-G. Jung, *J. Colloid Interface Sci.* **313**, 705 (2007).
- <sup>21</sup>S. T. Meyers, J. T. Anderson, C. M. Hung, J. Thompson, J. F. Wager, and D. A. Keszler, *J. Am. Chem. Soc.* **130**, 17603 (2008).
- <sup>22</sup>L. E. Greene, M. Law, D. H. Tan, M. Montano, J. Goldberger, G. Somorjai, and P. Yang, *Nano Lett.* **5**, 1231 (2005).
- <sup>23</sup>F. Ding, J. M. Smith, and H. Wang, *J. Org. Chem.* **74**, 2679 (2009).
- <sup>24</sup>F. Maran, D. Celadon, M. G. Severin, and E. Vianello, *J. Am. Chem. Soc.* **113**, 9320 (1991).
- <sup>25</sup>T. W. G. Solomons and C. B. Fryhle, *Organic Chemistry* (Wiley, 2008), p. 247.
- <sup>26</sup>K. Sarmini and E. Keddler, *J. Biochem. Biophys. Methods* **38**, 123 (1999).
- <sup>27</sup>J. W. Spalenka, E. M. Mannebach, D. J. Bindl, M. S. Arnold, and P. G. Evans, *Appl. Phys. Lett.* **99**, 193304 (2011).
- <sup>28</sup>H. S. Bae, M. H. Yoon, J. H. Kim, and S. Im, *Appl. Phys. Lett.* **83**, 5313 (2003).
- <sup>29</sup>Y. Liu, Z. Zhang, H. Xu, L. Zhang, Z. Wang, W. Li, L. Ding, Y. Hu, M. Gao, Q. Li, and L.-M. Peng, *J. Phys. Chem. C* **113**, 16796 (2009).
- <sup>30</sup>C.-S. Li, Y.-N. Li, Y.-L. Wu, B.-S. Ong, and F.-O. Loutfy, *J. Mater. Chem.* **19**, 1626 (2009).
- <sup>31</sup>A. E. Jimenez-Gonzalez, J. A. Soto Ureta, and R. Suarez-Parra, *J. Cryst. Growth* **192**, 430 (1998).
- <sup>32</sup>B. N. Pal, P. Trottman, J. Sun, and H. E. Katz, *Adv. Funct. Mater.* **18**, 1832 (2008).
- <sup>33</sup>J. F. Vig, *J. Vac. Sci. Technol. A* **3**, 1027 (1985).
- <sup>34</sup>W. M. Tang, M. T. Greiner, Z. H. Lu, W. T. Ng, and H. G. Nam, *Thin Solid Films* **520**, 569 (2011).
- <sup>35</sup>A. Hagfeldt, G. Boschloo, L. Sun, L. Kloo, and H. Pettersson, *Chem. Rev.* **110**, 6595 (2010).